Olefin Epoxidation by Molybdenum and Rhenium Peroxo and Hydroperoxo Compounds: A Density Functional Study of Energetics and Mechanisms

Philip Gisdakis, Ilya V. Yudanov,† and Notker Rösch*

Institut für Physikalische und Theoretische Chemie, Technische Universität München, 85747 Garching, Germany

Received February 20, 2001

A density functional study on olefin epoxidation by rhenium and molybdenum peroxo complexes has been carried out. Various intermediates and transition structures of the systems CH_3ReO_3/H_2O_2, H_3NMoO_3/H_2O_2, and H_3NOMoO_3/H_2O_2 were characterized, including ligated and unligated mono- and bisperoxo intermediates as well as hydroperoxo derivatives. For the rhenium system the bisperoxo complex $CH_3ReO(O_2)_2\cdot H_2O$ was found to be most stable and the one with the lowest transition state for epoxidation of ethylene (activation barrier of 16.2 kcal/mol), in line with experimental findings. However, participation of monoperoxo and hydroperoxo complexes in olefin epoxidation cannot be excluded. For both molybdenum systems, hydroperoxo species with an additional ammonia model ligand in axial position were calculated to be most stable. Inspection of calculated activation barriers of ethylene epoxidation reveals that, in both molybdenum systems, hydroperoxo mechanisms are competitive if not superior to peroxo mechanisms. The reaction barriers of the various oxygen transfer processes can be rationalized by structural, orbital, and charge characteristics, exploiting a model that interprets the electrophilic nature of the reactive oxygen center.

Introduction

Transition metal peroxo compounds play an important role in oxygen transfer to organic substrates such as olefins.[1] A well-studied example is methyltrioxorhenium (MTO) which is a highly efficient olefin epoxidation catalyst in the presence of hydrogen peroxide.[2] Herrmann et al.[3] showed that MTO reacts with H_2O_2 to form mono- and bis-peroxo complexes; the latter was found to be stabilized by an additional axial aquo ligand. Inorganic compounds such as ReO_4^- also activate peroxo compounds to convert olefins into epoxides.[4] Herrmann et al.[3] and Espenson et al.[5] have proposed reaction mechanisms for epoxidation involving either bisperoxo or monoperoxo derivatives of MTO. Structurally similar peroxo complexes of Mo(VI) and W(VI) constitute another important class of compounds active in the epoxidation of olefins.[6] Especially molybdenum peroxo complexes are used as stoichiometric reactants[7−9] and as catalysts.[10−13] While for rhenium complexes a peroxo intermediate seems to act as active oxygen source, there are strong indications that activated hydroperoxo groups are more reactive in other systems, e.g. for molybdenum peroxo complexes.[14] Very recently Wahl et al. showed that molybdenum bisperoxo complexes $MoO(O_2)_2(OER_3)$, with equatorial ligands OER_3 (E = N, P, As and R = *n*-dodecyl), are highly efficient olefin epoxidation catalysts.[13] Mechanistic aspects of olefin epoxidation with peroxo compounds were intensively studied during the last few years.[2,3,5] An interesting approach to the properties of oxygen transfer reactions, based on the sulfoxidation of thianthrene 5-oxide as mechanistic probe, was proposed by Adam and co-workers.[15−17] The electrophilic characteristics of V, Mo, and W peroxo complexes in oxygen transfer reactions were studied in similar fashion.[18−20]

The nature of the transition state of oxygen transfer from transition metal peroxo complexes to olefins has been under discussion for quite some time. Two models have been

* To whom correspondence should be sent.
† Permanent address: Boreskov Institute of Catalysis, Siberian Branch of the Russian Academy of Sciences, 630090 Novosibirsk, Russia.

(1) (a) Jacobsen, E. N. In *Catalytic Asymmetric Synthesis*; Ojima I., Ed.; VCH: New York, 1993; p 159. (b) Sheldon, R. A. *Catalytic Oxidations with Hydrogen Peroxides as Oxidant*; Kluwer: Rotterdam, 1992. (c) Jørgensen, K. A. *Chem. Rev.* **1989**, *89*, 431.
(2) (a) Herrmann, W. A. *J. Organomet. Chem.* **1995**, *500*, 149. (b) Herrmann, W. A.; Kühn, F. E. *Acc. Chem. Res.* **1997**, *30*, 169. (c) Romão, C. C.; Kühn, F. E.; Herrmann, W. A. *Chem. Rev.* **1997**, *97*, 3197.
(3) Herrmann, W. A.; Fischer, R. W.; Scherer, W.; Rauch, M. U. *Angew. Chem., Int Ed. Engl.* **1993**, *105*, 1209; *32*, 1157.
(4) Yudin, A. K.; Sharpless, K. B. *J. Am. Chem. Soc.* **1997**, *119*, 11537.
(5) Al-Ajlouni, A. M.; Espenson, J. H. *J. Am. Chem. Soc.* **1995**, *117*, 9243; *J. Org. Chem.* **1996**, *61*, 3969.
(6) Mimoun, H. In *Chemistry of Peroxides*; Patai, S., Ed.; Wiley: Chichester, 1983; p 463.
(7) Mimoun, H.; Seree de Roch, I.; Sajus, L. *Bull. Soc. Chim. Fr.* **1969**, *5*, 1481.
(8) Mimoun, H.; Seree de Roch, I.; Sajus, L. *Tetrahedron* **1970**, *26*, 37.
(9) Jørgensen, K. A.; Schiøtt, B. *Chem. Rev.* **1990**, *90*, 1483.
(10) Thiel, W. R.; Eppinger, J. *Chem. Eur. J.* **1997**, *3*, 696.
(11) Thiel, W. R. *J. Mol. Catal. A* **1997**, *117*, 449.
(12) Thiel, W.; Priermeier, T. *Angew. Chem., Int. Ed. Engl.* **1995**, *107*, 1870; *34*, 1737.
(13) Wahl, G.; Kleinhenz, D.; Schorm, A.; Sundermeyer, J.; Stowasser, R.; Rummey, C.; Bringmann, G.; Fickert, C.; Kiefer, W. *Chem. Eur. J.* **1999**, *5*, 3237.
(14) Thiel, W. R. *Chem. Ber.* **1996**, *129*, 575.
(15) Adam, W.; Dürr, H.; Hass, W.; Lohray, B. *Angew. Chem., Int. Ed. Engl.* **1986**, *98*, 85; *25*, 101.
(16) Adam, W.; Lohray, B. B. *Angew. Chem., Int. Ed. Engl.* **1986**, *98*, 185; *25*, 188.
(17) Adam, W.; Hass, W.; Lohray, B. B. *J. Am. Chem. Soc.* **1991**, *113*, 6202.
(18) Ballistreri, F. P.; Tomaselli, G. A.; Toscano, R. M.; Conte, V.; Di Furia, F. *J. Am. Chem. Soc.* **1991**, *113*, 6209.
(19) Bonchio, M.; Conte, V.; Assunta De Conciliis, M.; Di Furia, F.; Ballistreri, F. P.; Tomaselli, G. A.; Toscano, R. M. *J. Org. Chem.* **1995**, *60*, 4475.
(20) Adam, W.; Golsch, D.; Sundermeyer, J.; Wahl, G. *Chem. Ber.* **1996**, *129*, 1177.

10.1021/ic010201j CCC: $20.00
Published on Web 06/13/2001

suggested. One model assumes a direct attack of an olefin at a peroxo oxygen center, with a transition state of spiro structure.[21] At variance with this one-step mechanism, a two-step process has been proposed;[8] it implies an insertion of the olefin into a M−O bond in a [2+2]-like arrangement leading to a five-member metallacycle intermediate that involves two carbon atoms, the metal center, and a peroxo group. In this mechanism, the epoxide must be extruded from the metallacycle via a second transition state.

During the past decade quantum chemical calculations using density functional methods proved to be valuable tools for investigating olefin epoxidation by transition metal complexes. While early computational studies focused on structural aspects of MTO related oxo complexes,[22] we recently investigated the mechanism of olefin epoxidation, including the calculation of transition states, by transition metal peroxo complexes of Ti,[23] Cr, Mo, W[24] and Re.[25] Recently, the epoxidation of allylic alcohol by rhenium peroxo complexes has been investigated computationally with special focus on the role of hydrogen bonding between an alcohol substrate and a peroxo complex.[26] An important finding is that all these peroxo compounds with d^0 electron configuration at the transition metal center exhibit essentially the same epoxidation mechanism[23−27] which is also valid for organic peroxo compounds such as dioxiranes and peracids.[28,29] The calculations reveal that direct nucleophilic attack of the olefin at an electrophilic peroxo oxygen center via a transition state of spiro structure is preferred as significantly lower activation barriers were calculated for it than for the two-step insertion mechanism.[23−25] A recent computational study of epoxidation by Mo peroxo complexes showed that the metallacycle intermediate of the insertion mechanism leads to an aldehyde instead of an epoxide product.[30]

Despite of the common reaction mechanism, peroxo complexes exhibit very different reactivities depending on the particular structure, as shown by the calculated activation energies. We proposed a model[27,31] that is able to qualitatively rationalize differences in the epoxidation activities of a series of structurally similar transition metal peroxo compounds $CH_3Re(O_2)_2O{\cdot}L$ with various Lewis base ligands L. In this model the calculated activation barriers of direct oxygen transfer from a peroxo group to an olefin are correlated with the energies of pertinent orbitals, the π(C−C) HOMO of the olefin, and the σ^*(O−O) LUMO of the peroxo group.[31,32] When applied to organic peroxides, this rather simple model performs especially well.[33−35] Although most of the computational studies are limited to reactions in the gas phase, solvent effects on the activation barriers were investigated for organic peroxo compounds, dioxirane, and acetic percarboxylic acid.[33] The elaborated relationship between the solvent-induced change of the activation energy and the value of the solvent's dielectric constant ϵ was applied to estimate the solvent effect on the activity of $CH_3Re(O)(O_2)_2{\cdot}L$ (L = H_2O, pyridine, pyrazole).[33]

The goal of the present work is to compare at the same computational level the epoxidation activity of the following transition metal catalytic systems: CH_3ReO_3/H_2O_2, $H_3N{\cdot}MoO_3/H_2O_2$, and $H_3NO{\cdot}MoO_3/H_2O_2$. Starting with the trioxo precursors CH_3ReO_3 and $L{\cdot}MoO_3$ (L = NH_3, ONH_3), we concentrate on characterizing different peroxo derivatives that are formed via interaction of these precursors with H_2O_2 molecules. Broadening the scope of our previous work on peroxo complexes of Mo and Re,[24,25] here we will also address mechanisms of oxygen transfer involving hydroperoxo intermediates such as $CH_3ReO(O_2)(OH)(OOH)$ and $L{\cdot}MoO(O_2)(OH)(OOH)$. The activity of different peroxo intermediates will be discussed on the basis of the calculated energetics and activation barriers for oxygen transfer.

Reaction Models

Intermediates. The evolution of the system L_1MO_3 (M = Re, Mo) in the presence of H_2O_2 is schematically depicted in Figure 1. For rhenium L_1 is CH_3, while in the case of molybdenum we employ the model ligands NH_3 and ONH_3. Trioxo precursor complexes are designated as **1**, monoperoxo complexes formed from **1** via formal substitution of an oxo ligand by peroxo group are designated as **2**, and bisperoxo complexes, resulting from subsequent substitution of a further oxo ligand, as **3**. Complexes **1**−**3** can form the Lewis-base adducts which we denote as **B** while we use the designator **A** for the corresponding base-free complexes. Thus, in the following we will abbreviate trioxo compounds of the type L_1MO_3 as **1A**(Re), **1A**(Mo·NH_3), and **1A**(Mo·ONH_3). With **2A**(M) and **3A**(M) we will refer to the monoperoxo and bisperoxo complexes $L_1MO_2(O_2)$ and $L_1MO(O_2)_2$, respectively. Accordingly, the complexes $L_1L_2MO_3$, $L_1L_2MO_2(O_2)$, and $L_1L_2MO(O_2)_2$, with their additional base ligand L_2, will be labeled **1B**(M), **2B**(M), and **3B**(M), respectively. As ligand L_2 we use H_2O in the case of Re and an NH_3 molecule in the case of molybdenum complexes. Finally, the hydroperoxo derivatives $L_1MO(OOH)(OH)(O_2)$, **4A**(M) (Figure 1), and $L_1L_2MO(OOH)(OH)(O_2)$, **4B**(M), can formally be constructed by addition of a water molecule to a peroxo group of the bisperoxo complexes **3A**(M) and **3B**(M), respectively.

The analogy between Re and Mo systems is emphasized by the fact that the precursors $H_3C{\cdot}ReO_3$ and $H_3N{\cdot}MoO_3$ as well

(21) Sharpless, K. B.; Townsend, J. M.; Williams, D. R. *J. Am. Chem. Soc.* **1972**, *94*, 195.
(22) (a) Szyperski, T.; Schwerdtfeger, P. *Angew. Chem., Int. Ed. Engl.* **1989**, *101*, 1271; *28*, 1228. (b) Köstlmeier, S.; Pacchioni, G.; Herrmann, W. A.; Rösch, N. *J. Organomet. Chem.* **1996**, *514*, 111. (c) Köstlmeier, S.; Häberlen, O. D.; Rösch, N.; Herrmann, W. A.; Solouki, B.; Bock, H. *Organometallics* **1996**, *15*, 1872.
(23) Yudanov, I. V.; Gisdakis, P.; Di Valentin, C.; Rösch, N. *Eur. J. Inorg. Chem.* **1999**, 2135.
(24) (a) Di Valentin, C.; Gisdakis, P.; Yudanov, I. V.; Rösch, N. *J. Org. Chem.* **2000**, *65*, 2996. (b) Yudanov, I. V.; Di Valentin, C.; Gisdakis, P. Rösch, N. *J. Mol. Catal. A* **2000**, *158*, 189.
(25) Gisdakis, P.; Antonzcak, S.; Köstlmeier, S.; Herrmann, W. A.; Rösch, N. *Angew. Chem.* **1998**, *110*, 2331; *37*, 2211.
(26) Di Valentin, C.; Gandolfi, R.; Gisdakis, P.; Rösch, N. *J. Am. Chem. Soc.* **2001**, *123*, 2365.
(27) Rösch, N.; Gisdakis, P.; Yudanov, I. V.; Di Valentin, C. In *Peroxide Chemistry: Mechanistic and Preparative Aspects of Oxygen Transfer*; Adam, W., Ed.; Wiley-VCH: Weinheim, 2000; p 601.
(28) (a) Houk, K. N.; Liu, J.; DeMello, N. C.; Condroski, K. R. *J. Am. Chem. Soc.* **1997**, *119*, 10147. (b) Singleton, D. A.; Merrigan, S. R.; Liu, J.; Houk, K. N.; *J. Am. Chem. Soc.* **1997**, *119*, 3385. (c) Lucero, M. J.; Houk, K. N. *J. Org. Chem.* **1998**, *63*, 6973.
(29) (a) Bach, R. D.; Canepa, C.; Winter, J. E.; Blanchette, P. E. *J. Org. Chem.* **1997**, *62*, 5191. (b) Bach, R. D.; Estévez, C. M.; Winter, J. E.; Glukhovtsev, M. N. *J. Am, Chem, Soc.* **1998**, *120*, 680. (c) Bach, R. D.; Glukhovtsev, M. N.; Gonzales, C. *J. Am. Chem. Soc.* **1998**, *120*, 9902.
(30) (a) Deubel, D. V.; Sundermeyer, J.; Frenking, G. *J. Am. Chem. Soc*. **2000**, *122*, 10101. (b) Deubel, D. V.; Sundermeyer, J.; Frenking, G. *Inorg. Chem*. **2000**, *39*, 2314.
(31) Kühn, F. E.; Santos, A. M.; Roesky, P. W.; Herdtweck, E.; Scherer, W.; Gisdakis, P.; Yudanov, I. V.; Di Valentin, C.; Rösch, N. *Chem. Eur. J.* **1999**, *5*, 3603.
(32) For a discussion of the chemical interpretation of Kohn−Sham orbital energies, see: Görling, A.; Trickey, S. B.; Gisdakis, P.; Rösch, N. In *Topics in Organometallic Chemistry*; Brown, J., Hofmann, P., Eds; Springer: Heidelberg, 1999; Vol. 4, p 109.
(33) Gisdakis, P.; Rösch, N. *Eur. J. Org. Chem.* **2001**, 719.
(34) Gisdakis, P.; Rösch, N. *J. Phys. Org. Chem.*, in press.
(35) Kim, C.; Traylor, T. G.; Perrin, C. L. *J. Am. Chem. Soc*. **1998**, *120*, 9513.

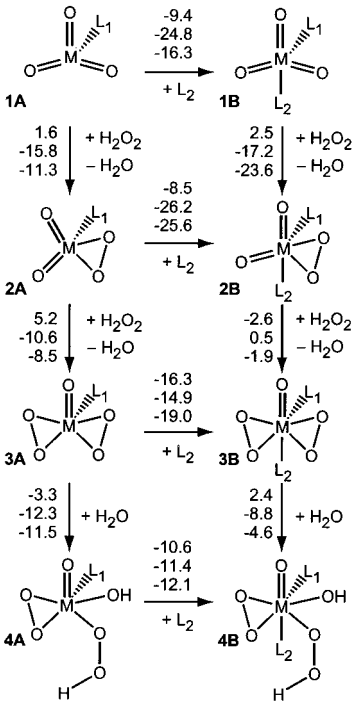

Figure 1. Schematic representation of structures and reaction energies ΔE (in kcal/mol) for the peroxidation and the base adduct formation of various transition metal complexes. The values of each column refer to M = Re, $L_1 = CH_3$, $L_2 = H_2O$ (top row); M = Mo, $L_1 = L_2 = NH_3$ (middle row); M = Mo, $L_1 = ONH_3$, $L_2 = NH_3$ (bottom row).

as the corresponding peroxo derivatives exhibit isoelectronic valence shell structures. We will also consider aminoxide ligands ONH_3 in the system $H_3NO{\cdot}MoO_3/H_2O_2$ to model a family of Mo complexes with ligands $O{=}ER_3$ (E = N, P, As) where R are long-chain alkyl substituents; these complexes are of great practical importance for olefin epoxidation.[13] In contrast to NH_3 the model ligand ONH_3, due to its more flexible connection to the complex, is able to form intra-complex hydrogen bonds with oxo and peroxo centers. To avoid artifacts of such intra-complex hydrogen bonds on the epoxidation activity of a peroxo complex we always consider those orientations of the ligand where the hydrogen atoms of ONH_3 do not directly interact with the peroxo group attacked by the olefin.

Reaction Mechanisms and Pathways. As mentioned in the Introduction, two mechanisms are being discussed for the epoxidation of olefins by transition metal peroxo complexes. The olefin is assumed to either directly attack a peroxo group or it is postulated to precoordinate at the metal center, followed by an insertion into a metal oxygen bond which results in a five-member metallacycle intermediate.[8] The spatial characteristics of the direct attack for either organic or metal peroxo intermediate were also under discussion[29,36] since in the transition state both planar and spiro approaches of the olefin double bond to the peroxo group are conceivable. Calculations revealed that for transition metal complexes spiro and planar transition structures with ethylene as model olefin exhibit moderate differences only, but the spiro orientation is always found to be preferred. For instance, for the monoperoxo complex CH_3-$ReO_2(O_2)$,[26] transition states with the ethylene double bond oriented in the plane of the Re-peroxo group are 3 to 5 kcal/mol higher in energy (depending on the reacting peroxo-oxygen center, "front" or "back", see below) than the corresponding transition states with spiro structure. Therefore, in the present work we consider direct attacks only via spiro transition states.

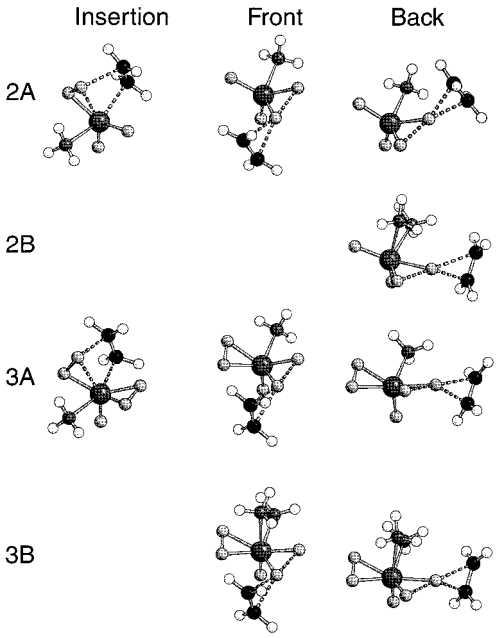

Figure 2. Transition state structures of ethylene epoxidation starting from the peroxo complexes **2A**, **2B**, **3A**, and **3B** of the system $Mo{\cdot}NH_3$ for insertion (**I**) as well as direct oxygen transfer via front-side spiro (**F**) and backside spiro (**B**) reaction pathways.

The oxygen centers of the peroxo group in most peroxo and all hydroperoxo intermediates under study are not symmetry equivalent. To characterize the calculated transition structures we will employ the following nomenclature. A direct attack of an olefin on a peroxo group may occur either from the front side (distant from the equatorial ligand L1, see Figure 1), denoted as "front" (**F**), or from the backside (proximate to the equatorial ligand), denoted as "back" (**B**).[25] Previous computational studies favored the direct attack, yielding evidence against the insertion mechanism.[24,25] Nevertheless, we present here also calculated activation energies for insertion processes (designated by **I**) to provide a complete overview of these mechanisms. To refer to a particular transition state we concatenate the symbol indicating the type of the transition structure and the corresponding designator of the starting complex; for instance, **F3B**(Re) (see Figure 2) denotes a transition state corresponding to direct front-side spiro attack of an olefin on the peroxo group of the water-stabilized rhenium bisperoxo complex **3B**(Re). (In context, no confusion should arise between the designators **B** for the transition state of a backside attack preceding the system number and for the base adduct following it.) Thus, up to 12 types of oxygen transfer processes (Figure 2) involving the peroxo intermediates **2A**, **2B**, **3A,** and **3B** have been considered for each $L_2L_1{\cdot}MO_3/H_2O_2$ system: 4 transition states of insertion and 8 transition states of direct attacks (front and back).

For hydroperoxo species the number of possible configurations of intermediates as well as transition structures increases since an OOH group features more conformational freedom than a peroxo group.[25] In particular, the metal hydroperoxo group $M{-}O_\alpha{-}O_\beta{-}H$ can be arranged in such a way that the α oxygen atom (closer to the metal center) is distal (front side orientation) or close (backside) to the equatorial ligand L_1; see the two configurations of **4A**(Re) in Figure 3. In the following, we present results only for the lowest energy configurations of the intermediates **4A** and **4B**, unless specified differently. The olefin

(36) Wu, Y.-D.; Lai, D. K. W. *J. Org. Chem.* **1995**, *60*, 673.

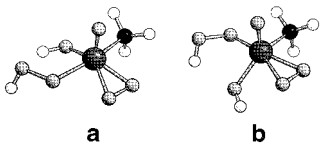

Figure 3. Two conformations of the hydroperoxo group of the intermediate **4A**(Re) suitable for an attack at the α oxygen center from (a) the front side and (b) the backside.

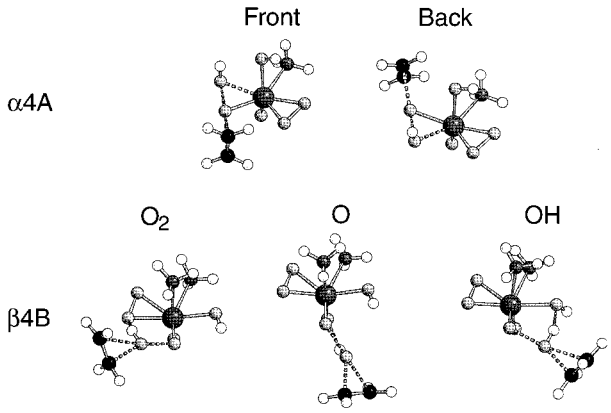

Figure 4. Transition state structures for different pathways of ethylene epoxidation by hydroperoxo complexes: α attack of **4A**(Mo·NH_3) with front and back orientation of hydroperoxo group; β attack of **4B**(Mo·NH_3) with subsequent proton transfer to peroxo (O_2), oxo (O), and hydroxo (OH) ligands as accepting group.

may interact with an α oxygen center of the metal hydroperoxo moiety or with a β oxygen center (carrying the proton) (Figure 4). In the case of an α attack, the OH group remaining after the O−O bond is broken has to be transferred back to the metal center. For a β attack, the proton may be transferred to one of several accepting groups. To limit the computational effort, we have investigated only intramolecular proton transfer, in analogy to commonly accepted transition structures for the olefin epoxidation with peracids.[28,29] Hydroperoxo intermediates exhibit three potentially protophilic sites, namely oxo, hydroxo, or peroxo groups; the corresponding transition states will be denoted by **O**, **OH**, or $\mathbf{O_2}$, respectively. For the α attack we investigated only pathways starting from complex **4A** since back transfer of the remaining OH group to the metal center is sterically strongly hindered if a Lewis-base ligand is coordinated to the metal center (**4B**) because the coordination sphere of the metal center is too crowded. The β attack was studied for complexes without (**4A**) and with (**4B**) an additional base ligand.

As we can see, any straightforward count of conceivable transition states for hydroperoxo species, especially in the case of a β attack, would easily result in dozens of possible structures. Molecular dynamics simulations of the whole reaction system are the method of choice for treating a problem with such a complex phase space; one would have to calculate a reasonably large number of trajectories and average over these results.[37] The key aspect of any molecular dynamics method is the description of the interatomic interactions. Molecular dynamics calculations with accurate forces are computationally extremely very demanding even for gradient-corrected exchange-correlation functionals.[38,39] For a similarly approach as presented here, namely the B3LYP hybrid density functional method (see "Computational Details"), we are not aware of any such study of a transition metal system.

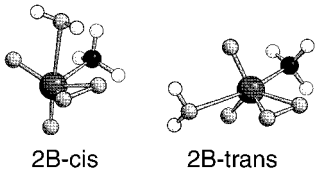

Figure 5. Cis and trans conformations of the ligands H_2O and CH_3 of the mono peroxo complex **2B**(Re).

In the following, we will use a conventional quantum chemical approach to investigate the mechanism of olefin epoxidation by peroxo complexes. On the basis of chemical reasoning, we judiciously selected a number of intermediates for which we characterized transition states. Nevertheless, in the following we will present a total of about 50 transition states for the three systems of interest. In this way we are able to describe pertinent features of the catalytic systems under investigation. It will turn out that often several pathways with transition states of comparable energy are available to the system, preventing the identification of a unique, preferred reaction pathway. Specific reaction conditions in a given experiment may affect the propensities of these alternative pathways.

Results and Discussion

Energetics of Intermediates. The reaction energies of the peroxidation reactions in the systems CH_3ReO_3/H_2O_2 and $H_3N{\cdot}MoO_3/H_2O_2$ have been separately analyzed elsewhere.[24a,25] Here, we briefly summarize these results comparing the Re and Mo systems, and we extend the analysis to the system $H_3NO{\cdot}MoO_3/H_2O_2$. In this comparison, we will also comment on the formation energetics of pertinent hydroperoxo species. The transformation energies (in kcal/mol) for all intermediates characterized starting from the trioxo precursors **1A** for Re and Mo are indicated in Figure 1.

Inspection of the reaction energies displayed in Figure 1 shows that all intermediates of the left-hand column form stable Lewis-base adducts. The stabilization energy ranges from −8.5 kcal/mol for **2A**(Re) → **2B**(Re) to −26.2 kcal/mol for **2A**(Mo·NH_3) → **2B**(Mo·NH_3). Interestingly, for bisperoxo, **3A**, and hydroperoxo, **4A**, intermediates the energies of base adduct formation for the Re complexes do not differ much from those of the analogous Mo complexes, although in the case of Re the Lewis base is H_2O whereas for Mo we used NH_3 and ONH_3 as model ligands. On the other hand, the Re trioxo, **1A**, and monoperoxo, **2A**, complexes exhibit significantly weaker bonds with an additional base ligand than the corresponding Mo species. Also, note that for **1B**(Re) and **2B**(Re) the cis conformation of CH_3 and H_2O ligands is by about 1 kcal/mol lower in energy than the trans conformation (see the cis and trans conformations of **2B**(Re) in Figure 5), while for the systems **1B**(Mo) and **2B**(Mo) the trans conformation of the bases L_1 and L_2 is the only one possible since the cis conformation is reduced to **1A**/**2A** and a separate NH_3 molecule during optimization.

The peroxidation process, i.e., the formal substitution of an oxo ligand by a peroxo group, tends to be almost isoenergetic for Re complexes, while a pronounced exothermic effect is

(37) (a) Haile, J. M. In *Molecular Dynamics Simulation: Elementary Methods*; Wiley: New York, 1997. (b) Frenkel, D.; Smit, B. *Understanding Molecular Simulation: From Algorithms to Applications*; Academic Press: New York, 1996.

(38) (a) Car, R.; Parrinello, M. *Phys. Rev. Lett.* **1985**, *55*, 2471. (b) Blöchl, P. E. *Phys. Rev. B* **1994**, *50*, 17953.

(39) (a) Senn, H. M.; Blöchl, P. E.; Togni, A. *J. Am. Chem. Soc.* **2000**, *122*, 4098. (b) Woo, T. K.; Blöchl, P. E. Ziegler, T. *J. Phys. Chem. A* **2000**, *104*, 121.

found for most species of both Mo families (Figure 1). The reaction energies of the systems (Mo·NH_3) and (Mo·ONH_3) are rather similar; for instance, for **1A**(Mo·ONH_3) → **3A**(Mo·ONH_3) the calculated overall peroxidation energy is −19.8 kcal/mol, while for **1A**(Mo·NH_3) → **3A**(Mo·NH_3) we obtained −26.4 kcal/mol. For the overall process **1A** → **3B**, transformation energies of −41.3 and −38.8 kcal/mol have been determined for the systems (Mo·NH_3) and (Mo·ONH_3), respectively. The addition (e.g. to **3A**) of the second "base" ligand is responsible for that major increase of stabilization when forming complexes **3B**.

For the system L·$MoO(O_2)_2$, the Mo-L binding energy is −44.9 kcal/mol for L = NH_3 and −63.5 kcal/mol for L = ONH_3, the difference being 18.6 kcal/mol. For the trioxo precursors $LMoO_3$ the difference between both Mo-L ligand binding energies is even larger, 23.3 kcal/mol (with binding energies of −54.8 kcal/mol for L = NH_3 and −78.1 kcal/mol for L = ONH_3). Thus, an aminoxide ligand stabilizes the Mo center better than an amine ligand.

As it is shown in Figure 1 the hydroperoxo intermediates **4A** and **4B** are obtained from bisperoxo complexes **3A** and **3B** by the opening of one of their peroxo rings. For the molybdenum complexes, this formal water addition process leads to the most stable species of the reaction system, **4A**(Mo·ONH_3) and **4B**(Mo·NH_3). The activation barrier of the ring opening reaction that transforms **3B**(Mo·NH_3) into **4B**(Mo·NH_3) has been calculated to 11.3 kcal/mol. Interaction of a peroxo complex with a hydrogen peroxide molecule can also lead to a hydroperoxo species.[14,40] Recall that in the Re system the complex **3B**(Re) is the most stable species; this complex has been characterized by X-ray analysis[3] and previously compared to the calculated structure.[25] Also for the molybdenum bisperoxo complexes, calculated and experimental structures compare satisfactorily.[24]

HOMO−LUMO Orbital Interaction Model. The early transition metal peroxo complexes behave as electrophilic oxidants, as for instance shown for complexes of V, Mo, and W using the thianthrene 5-oxide probe.[18−19,20] It is also known that epoxidation of electron-rich olefins, e.g., highly alkyl substituted species, exibits higher reaction rates. The electrophilic character of oxygen transfer can be rationalized by reference to a frontier orbital argument.[31] In the reaction between a peroxo complex and an olefin, the dominating interaction occurs between the π(C−C) HOMO of the olefin and the σ*-(O−O) LUMO of the peroxo group. The energy difference between these two orbitals controls the barrier differences for similar peroxo compounds.[28,31] The other frontier orbital interaction between the occupied π*(O−O) of the peroxo group and the unoccupied π*(C−C) of the olefin is less important for the determination of the activation barrier, although it seems to play a role in favoring the spiro structure of transition states over the planar structure.

To confirm the relevance of this orbital interaction to the determination of the epoxidation barrier we calculated the epoxidation transition states (all of them of spiro structure) of the model olefins ethylene, propene, *cis*-2-butene, 2-methyl-2-butene, and 2,3-dimethyl-2-butene for the bisperoxo compounds **3A**(Re), **3A**(Mo·NH_3), and **3A**(Mo·ONH_3). The calculated heights of the resulting epoxidation barriers vary linearly with the energy of the olefin HOMO (Figure 6). Similar findings have been obtained for organic oxygen donors such as dioxirane and peracids.[28,35] Each methyl substituent of the olefin pushes

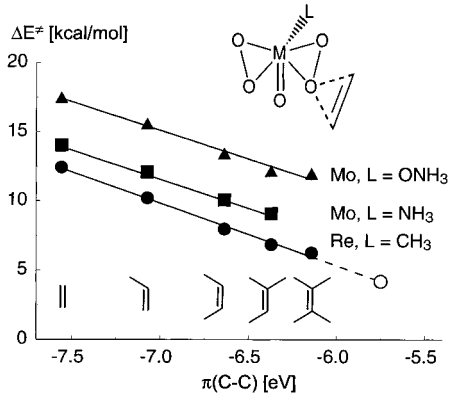

Figure 6. Calculated energy barriers $\Delta E^{\ddagger}$ (in kcal/mol) of the epoxidation of various substituted olefins (from left to right: ethylene, propene, *cis*-2-butene, 2-methyl-2-butene, and 2,3-dimethyl-2-butene) by the complexes **3A**(Re), **3A**(Mo·NH_3), and **3A**(Mo·ONH_3) as function of the energy of the olefin HOMO π(C−C). Also shown is the estimated reaction barrier of 4-methoxystyrene (empty circle), based on the corresponding HOMO energy.

electron density onto the C=C moiety and raises the olefin HOMO energy, thus increasing the interaction of the olefin with electrophilic oxidants. Concomitantly, the energy gap between the olefin HOMO and the peroxo LUMO decreases, entailing a lower activation barrier for epoxidation. Interestingly, the bisperoxo derivatives **3A** of the Re and Mo systems studied feature similar electrophilic behavior as indicated by the fact that all three lines shown in Figure 6 exhibit similar slopes.

We can apply this HOMO−LUMO model to predict reaction barriers of larger olefins without explicitly locating the transition state. As an example, we discuss the epoxidation of 4-methoxystyrene with the Re bis-peroxo complex **3B**(Re). The activation enthalpy has been measured to 10.2 ± 0.4 kcal/mol.[5] From the data displayed in Figure 6 and the calculated HOMO energy of 4-methoxystyrene, −5.75 eV, we extrapolate an activation barrier of about 4.2 kcal/mol when this substrate interacts with the intermediate **3A**(Re). By comparing the activation barriers of the direct front-side transition states of ethylene epoxidation by the complexes **3A**(Re) and **3B**(Re), 12.4 and 16.2 kcal/mol, respectively (see below), we estimate that water adduct formation increases the barrier height by 3.8 kcal/mol. Thus, our final estimate for the theoretical epoxidation barrier of 4-methoxystyrene is about 8.0 kcal/mol. This value is in good accordance with, but lower than, the experimental value,[5] although our theoretical estimate does not include solvent effects.

Activation Barriers Relative to the Direct Precursor. Epoxidation by Peroxo Complexes. In Table 1 we present the activation energies for ethylene epoxidation by various peroxo and hydroperoxo complexes. Calculated structural data of all precursor complexes and the corresponding transition states of direct oxygen transfer are provided as Supporting Information. Inspection of Table 1 reveals that for all complexes insertion transition states exhibit very high activation barriers. With one exception, activation barriers for insertion processes are always higher than the corresponding values for the direct oxygen transfer. The exception is the insertion transition state **I3A**(Mo·NH_3) with an activation energy of 22.3 kcal/mol which lies by 6.6 kcal/mol lower than **B3A**(Mo·NH_3). However, also in this case the direct mechanism is preferred since the attack of the *front* oxygen center **F3A**(Mo·NH_3) exhibits an activation barrier of only 14.1 kcal/mol. Therefore, in the following we will refrain from discussing the insertion mechanism.

(40) Hroch, A.; Gemmecker, G.; Thiel W. R. *Eur. J. Inorg. Chem.* **2000**, 1107.

Table 1. Calculated Activation Barriers $\Delta E^{\ddagger}$ (in kcal/mol) of Ethylene Epoxidation by Peroxo Complexes of Molybdenum and Rhenium for Various Reaction Pathways: Insertion **I**; Direct Oxygen Transfer from **2A**, **2B**, **3A**, and **3B** Complexes via Front-Side Spiro **F**, and Back-Side Spiro **B** Transition States; Direct Oxygen Transfer from Hydroperoxo Complexes **4A** and **4B**, Either Characterized as Front- or Back-Side α Oxygen Attack or as β Oxygen Attack with Various Hydrogen Acceptor Groups (Peroxo β**O$_2$4A**, Oxo β**O4A**, Hydroxo β**OH4A**)

	Mo			Re		
	I	**F**	**B**	**I**	**F**	**B**
2A	26.4	18.8 (18.5)	22.8 (19.8)	30.9	18.8	18.9
2B	*a*	34.1 (35.0)	34.1	*b*	*b*	16.2
3A	22.3 (23.0)	14.1 (15.5)	28.9 (21.3)	25.8	12.4	19.2
3B	*a*	19.7 (21.2)	27.5	38.7	16.2	23.3
α4A[c]		20.5 (16.5)			15.8	21.9
	O$_2$	**O**	**OH**	**O$_2$**	**O**	**OH**
***β*4A**	25.3 (29.2)	28.9 (27.0)	35.5 (25.3)	17.4	27.0	18.5
***β*4B**	27.5 (30.9)	31.6	30.3	21.2	21.5	17.8

Values in parentheses refer to molybdenum complexes with ONH_3 ligands. [a] No barrier available since the second ammonia ligand is expelled during the transition state search. [b] No transition state localized since the water ligand is expelled during the search. [c] For Re systems, the barriers are relative to intermediates with orientations of the hydroperoxo group suitable for attacks at the α oxygen center from the front and backside, respectively.

From Table 1 we recognize that for all bisperoxo intermediates attacks of peroxo groups from the front side require lower activation energies than the corresponding backside attacks. The situation is somewhat more complicated for monoperoxo complexes. In particular, the barrier heights of the transition states **F2A**(Re) and **B2A**(Re) are almost equal, about 19 kcal/mol. For the cis conformation of **2B**(Re) (Figure 5) the direct backside transition structure **B2B**(Re) (16.2 kcal/mol, Table 1) is the only one characterized whereas during the attempt to localize the transition structure **F2B**(Re) the additional water ligand is extruded from the complex during the oxygen transfer reaction. On the other hand, the trans conformation of **2B**(Re) (Figure 5), which is almost degenerate with the cis conformation, exhibits activation barriers of 20.2 and 23.9 kcal/mol for front and backside attacks, respectively, i.e., higher than the backside attack of the cis conformation. The low barrier of **B2B**(Re) is in line with the fact that the bond Re−O$_{back}$ of **2B,** 2.02 Å, is considerably longer than in **2A**, 1.97 Å.[25] Inspection of further structural data reveals (see the Supporting Information) that this backside metal−oxygen bond of intermediate **2B** is the longest Re−O(peroxo) distance among all rhenium complexes studied here. For the molybdenum system Mo·ONH_3, we also found very close activation energies for the processes **F2A** and **B2A**, 18.5 and 19.8 kcal/mol, respectively. Note that in the intermediate **2B**(Mo·NH_3) (analogous to **2B-trans**(Re), Figure 5) the peroxo oxygen centers are symmetry equivalent (C_{2v} symmetry); therefore there is no difference between front and backside attacks here.

The following general trends can be derived from a comparison of the lowest activation barriers (corresponding to a front attack for most species) calculated for peroxo intermediates **2A**/**2B** and **3A**/**3B** of the systems Re, Mo·NH_3, and Mo·ONH_3 (Table 1). (i) Re complexes exhibit slightly lower activation barriers than the corresponding Mo species. (ii) The base effect is considerably weaker for Re than for Mo complexes. For monoperoxo intermediates this trend is especially clear: in both Mo systems the activation energy of the base adduct **2B** is higher by about 16 kcal/mol than for the corresponding base-free complex **2A**, while **2B**(Re) yields even a lower activation barrier than **2A**(Re). (iii) Mo·NH_3 and Mo·ONH_3 peroxo derivatives exhibit very similar behavior although corresponding activation barriers of the system Mo·ONH_3 are by about 1 kcal/mol higher.

Epoxidation by Hydroperoxo Complexes. Next we turn to a discussion of the reactivity of hydroperoxo complexes. Similarly to Ti hydroperoxo species[23] the attack of the α oxygen center of the hydroperoxo group of **4A** intermediates requires less activation energy than the attack of the β oxygen center (Table 1). Since in the case of **4A**(Re) the two states with an orientation of the α oxygen center ready for a front-side or a backside attack (Figure 3) are very close in energy, we discuss here the activation energies of both conformations of this intermediate. The conformation suitable for a front-side attack (Figure 3a) exhibits a significantly lower activation barrier (15.8 kcal/mol) than that suitable for a backside attack (Figure 3b) for which an activation barrier of 20.5 kcal/mol is calculated. For the systems Mo·NH_3 and Mo·ONH_3 the conformation of species **4A** suitable for a front attack is definitely preferred, as the other conformation lies about 9 kcal/mol higher. Therefore, only the activation barriers corresponding to the lowest state of **4A** are given in Table 1 for Mo systems. The transition structures α**4A**(Mo·NH_3) and α**4A**(Mo·ONH_3) exhibit significantly different activation energies, 20.5 and 16.5 kcal/mol, respectively. As already mentioned, for steric reasons (due to an additional axial ligand) it is not feasible to calculate the α attack of **4B** complexes.

For an attack at the β oxygen center of a hydroperoxo group, we have confined our investigations to intramolecular proton transfer where the accepting group is part of the same complex. Therefore, three reaction pathways were considered for the β attack of hydroperoxo species where an oxo, a hydroxo, or a peroxo group, respectively, acts as proton acceptor. The transition states energies are expected to reflect the basicity strengths of the different proton acceptors. For complex **4A**(Re), the β attack with a subsequent proton transfer to the oxo group features the highest activation barrier, 27.0 kcal/mol (Table 1), while for the peroxo and hydroxo groups as proton acceptors much lower barriers of 18.5 and 17.4 kcal/mol are calculated (transition structures **O$_2$**β**4A** and **OH**β**4A**, respectively). This trend is in line with the estimated proton affinity of the corresponding oxygen center using the HF as probe:[34] the energies of the hydrogen bonds formed between the HF probe molecule and the oxo, peroxo, and hydroxo groups of **4A**(Re) are calculated to −6.5, −7.0, and −9.9 kcal/mol, respectively. The lowest activation barrier of β attack is calculated for the pathway where the most nucleophilic hydroxo center acts as proton acceptor. There is no linear correlation between the height of the activation barrier and the calculated HF binding energy to the selected proton accepting center. Thus, steric interactions are likely to affect the rearrangement of the hydroperoxo group (which is necessary to bring the proton close to the accepting oxygen center) in a significant manner, influencing the activation energies of the various routes of the β attack to a different degree.

This latter observation also holds for the barriers of β attacks at the corresponding Mo·NH_3 complexes (Table 1). For complex **4A**(Mo·NH_3) as precursor we calculated barriers of 25.3, 28.9, and 35.5 kcal/mol for peroxo, oxo, and hydroxo groups as proton acceptors, respectively. The barriers for β attacks at **4A**(Mo·NH_3) and **4B**(Mo·NH_3) are higher (some of them significantly) than those of the corresponding rhenium complexes. In addition we note that the energies of the two lowest-lying hydroperoxo

Table 2. Pertinent Characteristics of Peroxo (**3A**) and Hydroperoxo (**4A**) Intermediates and the Corresponding Transition States **F3A** and α**4A** of Olefin Epoxidation by Front-Side Direct Oxygen Transfer in the Systems Re, Mo·NH_3, and Mo·ONH_3 (Front-Side α Attack in the Hydroperoxo Systems)[a]

	Re		Mo·NH_3		Mo·ONH_3	
intermediate	**3A**	**4A**	**3A**	**4A**	**3A**	**4A**
d(O1−O2), Å	1.45	1.44	1.45	1.45	1.45	1.44
d(M−O1), Å	1.94	2.03	1.97	2.00	1.96	1.97
d(M−O2), Å	1.92	2.99	1.94	2.88	1.93	2.59
q(O1), e	−0.35	−0.44	−0.37	−0.43	−0.38	−0.37
q(O2), e	−0.34	−0.44	−0.42	−0.47	−0.38	−0.43
σ*(O−O), eV	−0.83	0.46	0.34	0.44	0.45	0.49
ΔE_0, kcal/mol	−50.2		−34.7		−36.0	−40.9
transition state	**F3A**	**α4A**	**F3A**	**α4A**	**F3A**	**α4A**
$\Delta E^{\ddagger}$, kcal/mol	12.4	15.8	14.1	20.5	15.5	16.5

[a] Bond distances, d, NBO charges, q, of oxygen centers (O1 = front-side or α oxygen center; O2 = backside or β oxygen center), and σ*(O−O) orbital energies of the intermediates as well as energies ΔE_0 of the epoxidation reaction and the corresponding activation barriers $\Delta E^{\ddagger}$.

transition states starting from complex **4B**(Mo·NH_3) appear in reverse order compared to **4B**(Re·OH_2), with proton transfer to the peroxo group featuring the lowest transition state; in the Re systems, proton transfer to the hydroxo group is preferred. The complex **4B**(Mo·ONH_3) also exhibits a very high activation energy for ethylene epoxidation. Only the transition state **$O_2\beta$4B** was calculated (associated with a barrier of 30.9 kcal/mol) since it had been shown to be the variant of β attacks of **4A**(Mo·NH_3) and **4B**(Mo·NH_3) complexes with the lowest activation barrier.

Factors Governing the Reactivity. To identify factors which influence the epoxidation activity of a transition metal peroxo complex, one can monitor the following three characteristics of transition metal peroxo or hydroperoxo moieties: (i) the M−O and O−O bond strengths, measured through the bond lengths (these bonds are to be broken during the oxygen transfer process), (ii) the electrophilic properties of the peroxo oxygen centers (e.g., as estimated by a population analysis), and (iii) the energy of the σ*(O−O) orbital.

To compare the three systems under study, CH_3ReO_3/H_2O_2, H_3NMoO_3/H_2O_2, and H_3NOMoO_3/H_2O_2, we choose the peroxo, **3A**, and hydroperoxo, **4A**, intermediates as well of the corresponding transition states **F3A** and α**4A** for front-side direct attack by an ethylene. Also, these reaction pathways exhibit the lowest (or almost the lowest) activation barriers; in addition, because of the structural similarity, these pathways facilitate a comparison of analogous peroxo and hydroperoxo complexes. A comparison of β attack processes based on these reactivity criteria is difficult since the various subsequent proton-transfer steps exhibit differences in barrier heights of up to 10 kcal/mol (see Table 1, system **4A**(Mo·NH_3)); these differences cannot be described within the criteria listed above. In Table 2, we present pertinent characteristics of the intermediates **3A** and **4A** as well of the corresponding transition state **F3A** and **F4A** for front-side direct attack by an ethylene. In recognition of the three reactivity criteria listed above, we have selected the following characteristics of the intermediates: the bond lengths O−O and M−O, the charges q(O) of the attacked oxygen center, and the energy of the σ*(O−O) orbital. Furthermore, we compare the barrier heights of olefin epoxidation and, if available, the energy ΔE_0 of the epoxidation reaction.

For the front-side direct transfer **F3A**, we identify the Re system as the one with the lowest activation energy (12.4 kcal/mol), followed by Mo·NH_3 (14.1 kcal/mol) and Mo·ONH_3 (15.5 kcal/mol). This ordering of the activation barriers is quite accurately reflected by the energy of the σ*(O−O) orbital as expected by the frontier orbital argument discussed previously: the higher the σ*(O−O) energy, the larger the activation energy. This holds even for complexes where the electronic structure is somewhat different; see the previous analysis of Ti hydroperoxo complexes.[23] The charge q(O) of the peroxo groups supports the proposed electrophilic character of the olefin attack at the metal peroxo moiety. More negative charges q(O) of the peroxo complexes are associated with higher activation barriers. However, the α attack in the hydroperoxo systems **4A** does not follow this trend.[23] Also the reaction energies ΔE_0 show, to some extent, the expected propensity. In general, a larger exothermicity (in absolute terms) is associated with a lower barrier height although there are exceptions (cf. **F3A** of Mo·NH_3 and Mo·ONH_3). Bond distances do not always exhibit the expected trends. For the hydroperoxo systems **4A**, longer, thus more activated, O−O and M−O bonds entail lower barriers; see in particular **F4A**(Mo·ONH_3). However, the structural changes of the peroxo complexes are probably too small (at most 0.01 Å) to allow a meaningful interpretation.

Table 3. Pairwise Comparison X/Y of Related Peroxo and Hydroperoxo Systems **2A**, **3A**, **3B**, and **4A** of Rhenium and Molybdenum and of Various Direct Oxygen Transfer Processes **F**, **B**, and α (α Attack)

		Re	Mo·NH_3	Mo·ONH_3
F2A/F3A	Δd(O−O), Å	0.011	−0.001(−)	−0.010(−)
	Δd(M−O), Å	0.037	0.029	0.046
	Δq(O), e	0.00	0.02	0.04
	$\Delta\sigma$*(O−O), eV	−0.36	−0.09	0.05(−)
	Δ^2E_0, kcal/mol	−3.6	−5.8	−4.3
	$\Delta^2E^{\ddagger}$, kcal/mol	−6.4	−4.7	−3.0
F3A/F3B	Δd(O−O), Å	−0.002	−0.002	−0.003
	Δd(M−O), Å	0.018(−)	0.003(−)	−0.022
	Δq(O), e	−0.03	−0.02	0.01(−)
	$\Delta\sigma$*(O−O), eV	1.10	0.48	0.61
	Δ^2E_0, kcal/mol	7.8	−11.3	−5.1
	$\Delta^2E^{\ddagger}$, kcal/mol	3.8	5.7	5.7
F3A/B3A	Δd(M−O), Å	−0.028	−0.027	−0.037
	Δq(O), e	0.01(−)	−0.05	0.00
	$\Delta^2E^{\ddagger}$, kcal/mol	6.8	14.8	5.8
F3A/α4A	Δd(O−O), Å	−0.011	0.008	−0.003
	Δd(M−O), Å	0.082(−)	0.038	0.007
	Δq(O), e	−0.08	−0.05(−)	−0.01(−)
	$\Delta\sigma$*(O−O), eV	−1.29	−0.10	−0.04
	Δ^2E_0, kcal/mol	*a*	*a*	−13.4
	$\Delta^2E^{\ddagger}$, kcal/mol	3.4	−1.1	1.5

Differences, $\Delta = Y - X$, of bond distances, d, NBO charges, q(O), of oxygen centers attacked by the olefin, and σ*(O−O) orbital energies of the intermediates as well as differences of energies ΔE_0 of the epoxidation reaction and the corresponding activation barriers $\Delta E^{\ddagger}$. Changes opposite to the expected trend as derived from $\Delta^2E^{\ddagger}$ are marked by minus signs (−). [a] Data not available.

In the first part of Table 3 we compare the direct front-side attacks **F2A** and **F3A** at the six-coordinated mono and bisperoxo complexes **2A** and **3A**, respectively. The bisperoxo intermediate **3A** exhibits a lower barrier than the corresponding monoperoxo complex **2A** in all three metal−ligand systems, but this energy difference decreases along the series Re, Mo·NH_3, and Mo·ONH_3: −6.4, −4.7, and −3.0 kcal/mol, respectively. This trend is nicely reflected by the changes of the M−O bond lengths: 0.037, 0.029, and 0.046 Å for Re, Mo·NH_3 and Mo·ONH_3,

respectively. The M−O distance of the complex **3A** is always larger. For Re and Mo·NH_3, the changes $\Delta\sigma^*$(O−O) of the orbital energies are, as expected, negative and decreasing from Re to Mo·NH_3: −0.36 eV and −0.09 eV, respectively. Also the system Mo·ONH_3 complies with that trend, but the rather small change of 0.05 eV of the σ^*(O−O) orbital energy which does not agree with the expectations based on the change $\Delta^2E^{\ddagger}$ indicates the limit of the present model considerations. In all three pairwise comparisons, lower activation barriers $\Delta E^{\ddagger}$ are associated with larger absolute values of the exothermicity ΔE_0.

The second part of Table 3 deals with the effect of base adduct formation for the example of bisperoxo complexes, **3A** vs **3B**, and the direct front-side attack by an ethylene, **F3A** vs **F3B**. Previously we showed[25,31] that Lewis-base adducts of **3B**(Re) exhibit higher activation barriers than the base-free parent complex. The donating effect of the base is reflected in a more negative charge of the oxygen center and in higher energies of the acceptor orbital σ^*(O−O). The variations of the M−O bond lengths do not follow any regular trend, while O−O bond lengths vary concomitantly with the heights of the activation barrier.

Next, we compare front- and backside direct processes **F** and **B** for compounds **3A**. In Table 3 we list only the characteristics Δq(O) and Δd(M−O) of the oxygen center attacked by the olefin; the other parameters are identical for the two processes because they refer to the same starting complex. For all three systems, the front-side pathway features significantly lower reaction barriers. The changes of the oxygen charge and the corresponding M−O distance are in line with the differences of the reactions barrier, with the exception of Δq(O) of the rhenium system. For Mo·NH_3 the energy barriers of both reaction pathways differ dramatically; for this system, the backside attack is strongly disfavored.[24a]

In the final part of Table 3 we compare two epoxidation mechanisms, the front-side attack **F3A** and the α attack α**4A**. For Re and Mo·ONH_3, the transition state **F3A** is preferred over α**4A**, while in the case of Mo·NH_3 the transition structure α**4A** yields a slightly lower barrier than **F3A**. Interestingly, most characteristics are in line with the calculated differences of the activation barriers. Exceptions are the charge distribution of the Mo systems and the M−O bond length in the case of Re. Compared to the previous cases, the values Δq(O) deviate significantly from the expected behavior (Table 3). Apparently, these charge effects are overcompensated by other factors, e.g., the large changes of the σ^*(O−O) orbital energy (Table 3).

According to the results discussed so far, the reactivity of similar peroxo complexes correlates with the electrophilicity of the attacked oxygen centers. The orbital energy of the σ^*(O−O) level may serve as a criterion for both quantities, electrophilicity and reactivity. Clearly, the σ^*(O−O) orbital energy cannot be used to differentiate between the two oxygen centers of a given peroxo group. Rather, the proton affinity ΔE_{PA} of each oxygen center, an observable in principle, comes to mind as an obvious choice for this purpose. To probe this quantity, we calculated the adduct formation energy of HF as proton donor. In Figure 7 we display the activation energies $\Delta E^{\ddagger}$ of some transition structures as a function of the HF binding energy ΔE(HF). As expected, the reaction barriers drop with decreasing exothermicity values of the HF addition, i.e., with decreasing proton affinity or increasing electrophilicity of the oxygen center under study. Rhenium complexes clearly exhibit the expected correlation. For the molybdenum complexes this reactivity criterion is able to rationalize the reactivity differences within one system, e.g., between **B3A**(Mo·ONH_3) and **F3A**(Mo·ONH_3), but it apparently does not reflect the calculated reactivity differences between the systems Mo·ONH_3 and Mo·NH_3. As pointed out previously,[31] the reactivity of a transition metal complex is too complex a property to be monitored by a single criterion, such as the proton affinity. In this respect, organic peroxo compounds behave much more regularly; dioxirane exhibits an obvious correlation between the energy of HF addition and the activation barrier of olefin epoxidation.[34]

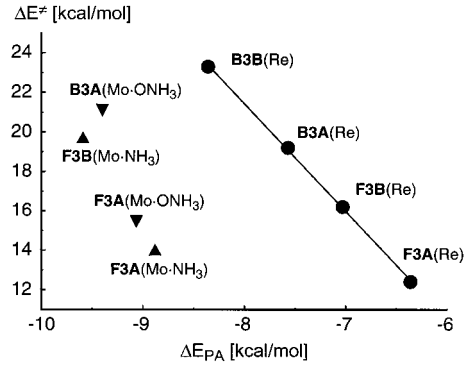

Figure 7. Calculated energy barriers $\Delta E^{\ddagger}$ (in kcal/mol) of ethylene epoxidation by various transition metal peroxo complexes as function of the proton affinity ΔE_{PA} of the attacked oxygen site as measured by the energy of HF addition (in kcal/mol).

In summary, the characteristics of intermediates as selected in Table 3 indeed have been found to allow a rationalization of the corresponding epoxidation barriers, for both peroxo and hydroperoxo complexes. However, while the reactivity of the various complexes can be reasonably well characterized in this way, one has to note exceptions for all reaction mechanisms and pathways.

Barriers Relative to a Common Precursor. To discuss the overall optimal reaction pathway we have to refer all transition states to a common starting system. A transition state might have a rather low activation barrier relative to its immediate precursor; however, if this precursor is not stable, e.g., if its formation is highly endothermic with respect to other species, the system will not react via this pathway. As an example we recall[31] that the process **F3A**(Re) has an activation energy of 12.4 kcal/mol, while the corresponding process **F3B**(Re) for a complex with an additional water ligand features a higher barrier of 16.2 kcal/mol (Table 1). However, since complex **3A**(Re) is 16.3 kcal/mol less stable than **3B**(Re) (Figure 1), transition state **F3B**(Re) still characterizes the preferred reaction pathway.[3]

In Figures 8, 9, and 10 we compare the energies of the various transition states determined for the systems CH_3ReO_3/H_2O_2, H_3NMoO_3/H_2O_2, and H_3NOMoO_3/H_2O_2, respectively, using complexes **3B** as a common energy reference of all intermediates and transition states.

The System CH_3ReO_3/H_2O_2. We begin by discussing the system MTO/H_2O_2 (Figure 8). Complex **4B**(Re), experimentally not characterized, is only 2.4 kcal/mol less stable than **3B**(Re) which we found to exhibit the lowest energy. Similar to **4B**(Re), complex **2B**(Re) is 2.6 kcal/mol less stable than **3B**(Re).

A Lewis-base ligand stabilizes a metal complex and may therefore also stabilize the corresponding transition states (on this absolute energy scale) although to a smaller extent.[31] While base-free transition states can be reached from their immediate precursor via lower activation barriers, the missing stabilization yields transition states of higher total energies.[31] The results compiled in Figure 8 corroborate this analysis. Complexes **2A**(Re), **3A**(Re), and **4A**(Re) without a stabilizing Lewis-base ligand lead to transition states that lie 10−15 kcal/mol higher

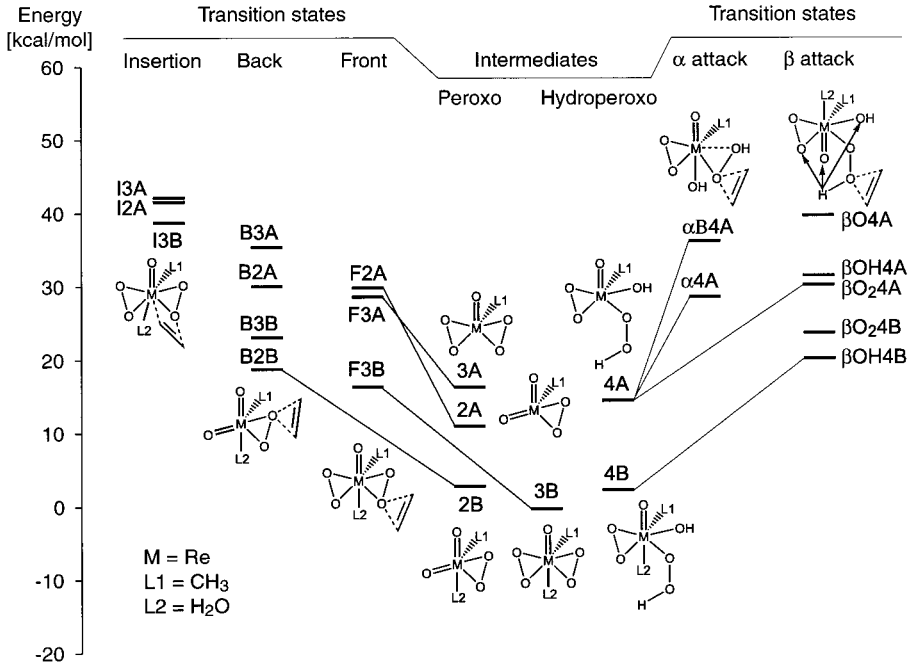

Figure 8. Energies (in kcal/mol) of intermediates and transition states of ethylene epoxidation by various rhenium peroxo and hydroperoxo complexes with respect to the common energy reference of the complex $CH_3ReO(O_2)_2 \cdot H_2O$ **3B**.

than those reached from the more stable, ligated complexes **2B**(Re), **3B**(Re), and **4B**(Re). Therefore, the former intermediates are not expected to play a significant role in the epoxidation reaction of MTO/H_2O_2.

The transition states of insertion processes all lie about 40 kcal/mol above the reference **3B**(Re); their energies are the highest of the Re system. On the basis of this finding we refrained from characterizing the subsequent reaction step in which the epoxide is eliminated from the metallapentacycle.

All other transition states characterized feature a direct attack of one of the oxygen atoms of a peroxo or a hydroperoxo group by the olefin. Front-side direct mechanisms tend to have lower absolute barriers than the corresponding backside processes, but the differences are rather small. On the absolute energy scale, the transition state **F3B**(Re) has the lowest energy (16.2 kcal/mol); **B2B**(Re) lies only slightly higher, at 18.8 kcal/mol. The relatively low absolute energy of **B2B**(Re) is due to the smaller activation energy of **2B**(Re) compared to **3B**(Re).

Inspection of the right-hand side of Figure 8 also reveals that reaction pathways which start from hydroperoxo complexes without a stabilizing Lewis-base ligand proceed via high-lying transition states. Recall that the α attack starts with the complex **4A** since the remaining hydroxo moiety of the attacked hydroperoxo group has to be transferred back to the metal center. For steric reasons this latter step is not feasible if a base is coordinated to the metal center; both α attack transition states exhibit quite high energies, 28.8 and 36.4 kcal/mol for front- and backside attack, respectively. The situation is similar for a β attack of **4A**(Re). For the oxo group as proton acceptor the corresponding transition state lies at 40.1 kcal/mol, while the β**OH4A** and β**O**$_2$**4A** transition structures exhibit energies of 31.6 and 30.4 kcal/mol, respectively. On the other hand, β attacks of the base-stabilized hydroperoxo complex **4B**(Re) yield transition states of moderate energies: 20.2, 23.6, and 23.9 kcal/mol for the processes β**OH4A**, β**O**$_2$**4A**, and β**O4A**, respectively. The first of these transition states lies only 4 kcal/mol higher in energy than the most stable transition structure of **F3B**(Re) with 16.2 kcal/mol. Thus, extending an earlier analysis,[25] we conclude that hydroperoxo complexes may play a certain role in the system MTO/H_2O_2.

Summarizing the results for the Re system MTO/H_2O_2, we find that the direct front-side attack of a water stabilized bisperoxo complex **3B** indeed leads to the transition structure with the lowest energy,[3,25] but a backside direct attack of the ligated monoperoxo complex **2B** may be competitive, depending on details of the experimental conditions.[5] Even the transition state for attack at an β oxygen center of the hydroperoxo complex **4B** with subsequent intramolecular proton transfer to a hydroxo group (i.e., formation of a water ligand) does not lie much higher in energy.

The System H_3NMoO_3/H_2O_2. The system H_3NMoO_3/H_2O_2 (Figures 9) shows a significant similarity to MTO/H_2O_2, although there are specific differences to note. In contrast to the system MTO/H_2O_2, the hydroperoxo complex **4B**(Mo·NH_3) is by far the most stable intermediate of this system, 8.8 kcal/mol below the bisperoxo species **3B**(Mo·NH_3). Also the intermediate **4A**(Mo·NH_3) lies only 3.6 kcal/mol higher than **3B**(Mo·NH_3). The monoperoxo intermediate **2B**(Mo·NH_3) is almost isoenergetic with **3B**(Mo·NH_3); the energy difference of 0.5 kcal/mol is at the limit of computational accuracy.

Just as for the Re system, insertion processes have very high barriers, 37.2 kcal/mol for **I3A**(Mo·NH_3) and 51.9 kcal/mol for **I2A**(Mo·NH_3). Thus, we have to reject this mechanism which had originally been proposed for molybdenum peroxo complexes.[8]

At variance with the system MTO/H_2O_2, one can rule out that the monoperoxo intermediate **2B**(Mo·NH_3) participates in the olefin epoxidation since it exhibits an extremely high activation barrier of 34.1 kcal/mol. At the absolute scale this state lies even higher than the transition states **F3A** and α**4A** which are reached from the less stable intermediates **3A** and **4A**, respectively (Figure 9).

Another difference from the system MTO/H_2O_2 is that there are two low-lying transition states, **F3B**(Mo·NH_3) and βO$_2$**4B**-(Mo·NH_3), with the energies of 19.7 and 18.7 kcal/mol, respectively, at the absolute scale. The activation barrier for

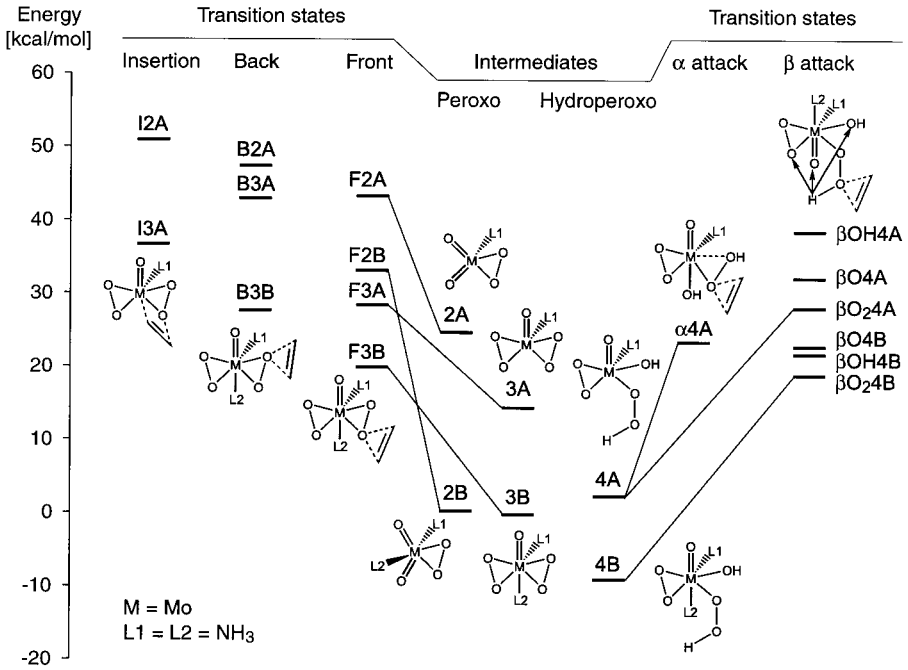

Figure 9. Energies (in kcal/mol) of intermediates and transition states of ethylene epoxidation by various molybdenum peroxo and hydroperoxo complexes with respect to the common energy reference of the complex $H_3N{\cdot}MoO(O_2)_2{\cdot}NH_3$ **3B**.

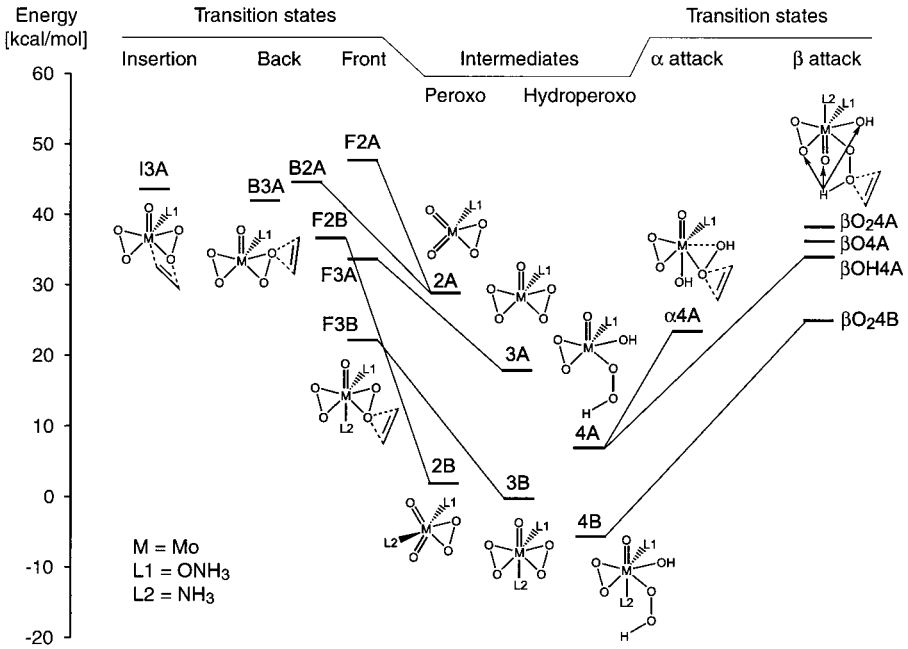

Figure 10. Energies (in kcal/mol) of intermediates and transition states of ethylene epoxidation by various molybdenum aminoxide peroxo and hydroperoxo complexes with respect to the common energy reference of the complex $H_3NO{\cdot}MoO(O_2)_2{\cdot}NH_3$ **3B**.

F3B(Mo·NH_3) is by 3.5 kcal/mol higher than the corresponding value for the transition state **F3B**(Re). On the other hand, transition state βO_2**4B**(Mo·NH_3) which corresponds to an attack at the β-oxygen center lies at a low absolute energy because of the higher stability of the preceding intermediate **4B**(Mo·NH_3) while the corresponding activation barrier is much higher (27.5 kcal/mol) than that of the corresponding process of the Re system. The relative stability of the complexes **3B**(Mo·NH_3) and **4B**(Mo·NH_3) may be sensitive to environmental effects that were not taken into account in our models. Nevertheless, the hydroperoxo epoxidation pathway suggested by Thiel based on experimental findings[14] seems to be competitive to epoxidation by peroxo complexes. Thus, instead of a direct front-side transfer, the molybdenum bisperoxo complex **3B**(Mo·NH_3) can react with water (or H_2O_2)[14] to form complex **4B**(Mo·NH_3). The activation barrier for such a ring opening reaction has been calculated to 11.3 kcal/mol. In addition, we note that the transition state α**4A** lies only 4.4 kcal/mol higher than **F3B**.

At this point we would like to refer to the available experimental data on the reactivity of Mo peroxo complexes. Experimental studies from the pioneering work of Mimoun[8] to the most recent investigations[13] provide unambiguous evidences that oxygen transfer from seven-coordinated Mo bisperoxo complexes such as **3B** is significantly slowed or even inhibited. Thus, the calculated activation barrier of about 20 kcal/mol for **F3B**(Mo·NH_3) seems to be beyond the threshold where Mo peroxo complexes are still reactive; one has to take into account that in our model we used the rather strong model base NH_3

which significantly reduces the activity of the peroxo group. In our model, the most probable pathway is that of a direct front-side attack of **3A**($Mo{\cdot}NH_3$) (with an activation barrier of 14.1 kcal/mol)—provided that reaction conditions are such that they prevent the coordination of a second strong base to this species.[13]

The System H_3NOMoO_3/H_2O_2. The energy pattern of the various intermediates and transition states of the system H_3NOMoO_3/H_2O_2 (Figure 10) resembles that of the Mo system with amine ligands (Figure 9). Here, the energies of hydroperoxo intermediates **4A** and **4B** with respect to **3B** are shifted upward by 4−5 kcal/mol compared to the energies of the corresponding states of the system $Mo{\cdot}NH_3$. The lowest transition state, at an absolute energy of 21.2 kcal/mol, corresponds to a front attack of the bisperoxo complex **3B**. It is interesting to note that the next higher transition state, at 24.0 kcal/mol on the absolute scale, is α**4A** corresponding to the transfer of an α oxygen from the hydroperoxo species **4A**, while the lowest-lying transition state starting from the more stable intermediate **4B** occurs at 26.3 kcal/mol on the absolute energy scale. Thus, the hydroperoxo **4A** pathway is obviously competitive with bisperoxo pathways at the absolute scale as well as with respect to individual intermediates; this finding supports earlier suggestions of Thiel.[14]

Summary

We have characterized various intermediates and transition structures of three transition metal peroxo systems CH_3ReO_3/H_2O_2, H_3NMoO_3/H_2O_2, and H_3NOMoO_3/H_2O_2 using a hybrid density functional approach. As potentially reactive species we have studied ligated and unligated mono and bisperoxo intermediates as well as hydroperoxo derivatives. For the rhenium system we found the bisperoxo complex $CH_3ReO(O_2)_2{\cdot}H_2O$ to be most stable within the reaction system, in line with experimental findings. This complex is also the most reactive one with the lowest-lying transition state and an activation barrier of 16.2 kcal/mol. However, monoperoxo and hydroperoxo complexes may also play a role in olefin epoxidation. For both molybdenum systems we found the hydroperoxo species to be more stable than the peroxo complexes: in the case of H_3NMoO_3/H_2O_2 the hydroperoxo derivative with an additional axial Lewis-base ligand is about 9 kcal/mol more stable than the corresponding bisperoxo complex. The most stable Mo intermediates (of peroxo and hydroperoxo type) exhibit significantly higher activation barriers than their Re counterparts. Inspection of the energy pattern of the various intermediates and transition states for molybdenum systems reveals that the hydroperoxo mechanisms is competitive, if not superior to the peroxo mechanisms. Exploiting the electrophilic character of the oxygen center attacked by the olefin, the reaction barriers of the individual processes have been rationalized by structural, orbital, and charge parameters of the immediate precursor complexes.

Computational Details

All electronic structure calculations were performed with the hybrid B3-LYP[41] density functional scheme[42] using effective core potentials for the metal centers Re and Mo.[43] For all other centers, a 6-311G(d,p) basis set was employed.[44] Geometry optimizations were carried out without any symmetry restrictions. Finally, two *f* exponents were added to the basis set of Mo and Re to evaluate energies in single-point fashion.[24,25] Details of this computational strategy have been discussed elsewhere.[45] Since the present study focuses on trends and their rationalization, we refrained from correcting stabilization energies and reaction barriers for enthalpy and solvent effects. Previous investigations have shown that such corrections (at least for similar Re compounds) do not affect the trends analyzed in the present study.[25,45] Charges of atoms were determined by a natural bond order analysis. Detailed results are presented as Supporting Information.

Acknowledgment. N.R. would like to thank W. A. Herrmann for bringing the problem of olefin epoxidation to his attention. During these investigations we have profited from discussions with S. Antonczak, C. Di Valentin, S. Köstlmeier, F.E. Kühn, P. Hofmann, H. Rothfuss, J.H. Teles, and W. Thiel. This work has been supported by the Deutsche Forschungsgemeinschaft, the Bayerische Forschungsstiftung (FORKAT), the Fonds der Chemischen Industrie, and INTAS-RFBR (Grant IR-97-1071). I. Yu. is grateful for support from the Siberian Branch of the Russian Academy of Sciences.

Supporting Information Available: Tables of selected geometry characteristics of calculated intermediates and transition states, activation barriers, and reaction energies. This material is available free of charge via the Internet at http://pubs.acs.org.

IC010201J

(41) (a) Becke, A. D. *J. Chem. Phys.* **1993**, *98*, 5648. (b) Lee, C.; Yang, W.; Parr, R. G. *Phys. Rev. B* **1988**, *37*, 785.
(42) Frisch, M. J.; Trucks, G. W.; Schlegel, H. B.; Gill, P. M. W.; Johnson, B. G.; Robb, M. A.; Cheeseman, J. R.; Keith, T.; Petersson, G. A.; Montgomery, J. A.; Raghavachari, K.; Al-Laham, M. A.; Zakrzewski, V. G.; Ortiz, J. V.; Foresman, J. B.; Cioslowski, J.; Stefanov, B. B.; Nanayakkara, A.; Challacombe, M.; Peng, C. Y.; Ayala, P. Y.; Chen, W.; Wong, M. W.; Andres, J. L.; Replogle, E. S.; Gomperts, R.; Martin, R. L.; Fox, D. J.; Binkley, J. S.; Defrees, D. J.; Baker, J.; Stewart, J. P.; Head-Gordon, M.; Gonzalez, C.; Pople, J. A. *Gaussian 94*, Revision D.4; Gaussian, Inc.: Pittsburgh, PA, 1995.
(43) (a) Hay, P. J.; Wadt, W. R.; *J. Chem. Phys.* **1985**, *82*, 299. (b) Frenking, G.; Antes, I.; Böhme, M.; Dapprich, S.; Ehlers, A. W.; Jonas, V.; Neuhaus, A.; Otto, M.; Stegmann, R.; Veldkamp, A.; Vyboishchikov, S. F. In *Reviews in Computational Chemistry*; Lipkowitz, K. B., Boyd, D. B., Eds.; VCH: New York, 1996; Vol. 8, p. 63.
(44) a) Krishnan, R.; Binkley, J.; Seeger, R.; Pople, J. *J. Chem. Phys.* **1980**, *72*, 650; b) McLean, A.; Chandler, G. *J. Chem. Phys*. **1980**, *72*, 5639.
(45) Gisdakis, P.; Antonczak, S.; Rösch, N. *Organometallics* **1999**, *18*, 5044.